

Anderson localization of light by impurities in a solid transparent matrix

S.E. Skipetrov*

Univ. Grenoble Alpes, CNRS, LPMMC, 38000 Grenoble, France

I.M. Sokolov†

Peter the Great St. Petersburg Polytechnic University, 195251 St. Petersburg, Russia

(Dated: August 5, 2024)

A solid transparent medium with randomly positioned, immobile impurity atoms is a promising candidate for observation of Anderson localization of light in three dimensions. It can have low losses and allows for mitigation of the detrimental effect of longitudinal optical fields by an external magnetic field, but it has its own issues: thermal oscillations of atoms around their equilibrium positions and inhomogeneous broadening of atomic spectral lines due to random local electric fields. We show that these complications should not impede observation of Anderson localization of light in such materials. The thermal oscillations hardly affect light propagation whereas the inhomogeneous broadening can be compensated for by increasing the number density of impurity atoms.

Anderson localization—a complete halt of wave transport due to disorder [1]—turns out to be difficult [2–11] and likely even impossible [12] to reach for light in fully disordered three-dimensional (3D) dielectric media. Partially ordered structures such as disordered photonic crystals [13–15] or hyperuniform materials [16, 17] featuring a photonic band gap may be required to obtain spatially localized optical modes at frequencies near a band edge where the optical density of states is strongly suppressed. Metallic structures may be better suitable for observation of Anderson localization of light than dielectric ones [12, 18] although real metals suffer from significant losses that can make optical experiments difficult to conduct and interpret [18, 19].

Cold atoms exhibiting purely elastic, lossless scattering have been proposed as an alternative medium for observation of Anderson localization of light in 3D without relying on photonic band gap effects [20, 21]. However, longitudinal electric fields have been later predicted to prevent such an observation [22, 23]. A possible solution to this problem consists in placing the atoms in a strong external magnetic field that partially suppresses longitudinal fields [24, 25]. Theoretical work has predicted the expected signatures of Anderson localization for coherent laser light in optically thick and dense cold-atom ensembles placed in a strong external magnetic field: slowing down of the temporal decay of a transmitted pulse [26], enhanced fluctuations of scattered intensity [27], step-like profile of average intensity inside the atomic sample [28]. However, the experimental realization of these theoretical predictions is currently impeded by the following two main obstacles. First, it is difficult to prepare cold-atom samples that would be optically thick to ensure multiple scattering (size $L >$ photon mean free path ℓ) and, at the same time, sufficiently dense to reach Anderson localization (atomic number density $\rho > \lambda_0^{-3}$, where λ_0 is the resonance wavelength in the free space) [21, 29]. Second, experiments are necessarily performed at a low but finite temperature (typically, $T \sim 100 \mu\text{K}$ [29, 30]) leading to residual motion of atoms that is likely to wash out interference phenomena in general and Anderson localization in particular [26, 31].

A transparent solid medium with impurity atoms or ions embedded at random locations is an alternative physical system described by the theoretical model of immobile point-like scattering centers (atoms or ions) developed in Refs. [22–26] and exhibiting the phenomenon of Anderson localization. Well-known examples of such materials are uranium glass (with U atoms in, e.g., oxide diuranate form as impurities) [32] and ruby (with Cr^{3+} ions as impurities), for which the possibility of Anderson localization of optical excitations have been already evoked [33, 34]. Another example is the diamond crystal with multiple nitrogen-vacancy centers—a system with promising application in quantum information science [35, 36]. Such media have a number of advantages as compared to cold atomic gases as far as the observation of Anderson localization of light is concerned. On the one hand, they can be found in nature or fabricated without fundamental limitations on the medium size L or impurity number density ρ , so that the conditions $L > \ell$ and $\rho > \lambda_0^{-3}$ can be readily fulfilled. On the other hand, experiments can be performed at room or, in any case, not-too-low temperature because impurities are fixed at their positions in the matrix and do not fly away. Two problems arise nevertheless in these systems. First, local electric fields induce position-dependent shifts of resonance frequencies of impurity atoms, driving them out of resonance with each other. Such an inhomogeneous broadening of the spectrum is expected to reduce the maximum achievable scattering strength, which may bring the system away from the Anderson localization regime. Second, the problem of atomic motion that is crucial in atomic gases, does not disappear completely here either: the solid matrix still allows for oscillations of impurity atoms about their equilibrium positions with an amplitude and a frequency determined by the temperature. At the first glance, such oscillations could be expected to be less detrimental for Anderson localization of light than the free atomic motion, but it is not clear to which degree. Thus, it is not clear *a priori* whether the replacement of free atomic motion by oscillations brought about by embedding the atoms in a solid host medium outweighs the detrimental impact of random local fields

due to the very same host medium and makes Anderson localization achievable under realistic conditions.

In the present Letter we analyze a theoretical model including both the oscillations of impurity atoms about their equilibrium positions and random frequency shifts of atomic energy levels. Our analysis predicts that Anderson localization of light should be achievable in random ensembles of impurity atoms embedded in a transparent solid host medium at finite temperatures. In particular, the fast but small-amplitude oscillations of impurity atoms around their equilibrium positions have virtually no effect on light propagation, in analogy with Dicke narrowing of Doppler broadened spectral lines in the presence of atomic collisions [37]. In contrast, the inhomogeneous broadening of atomic spectral lines does suppress scattering and makes Anderson localization more difficult to reach. However, this suppression can be compensated by increasing the number density of atoms, so that a photon mobility edge always exist, whatever the broadening.

We start with a standard Hamiltonian \hat{H} describing the free electromagnetic field coupled with N identical two-level atoms located at positions $\{\mathbf{r}_n\}$ and having each a ground state $|g\rangle$ with energy E_g and angular momentum $J_g = 0$, three degenerate excited states $|e_m\rangle$, $m = 0, \pm 1$, with energy $E_e = E_g + \hbar\omega_0$ and angular momentum $J_e = 1$, and the dipole moment $\mathbf{d}_{e_m g}$ of the transition $|g\rangle \rightarrow |e_m\rangle$ [38, 39]. Symmetry considerations impose $|\mathbf{d}_{e_m g}| = d$ independent of m . We follow the now well-known procedure to eliminate field variables and obtain an effective non-Hermitian Hamiltonian \hat{H}_{eff} describing immobile atoms coupled by the quasi-resonant electromagnetic field [40, 41]. When the lifting of the degeneracy of the excited state by an external magnetic field $\mathbf{B} = B\mathbf{e}_z$ and the inhomogeneous broadening of atomic spectral lines $\omega_n = \omega_0 + \Delta_n$ are included in the model, the effective Hamiltonian is composed of $N \times N$ blocks of size 3×3 that in units of $\hbar\Gamma_0/2$ can be written as

$$\begin{aligned} (\hat{H}_{\text{eff}})_{nn'} &= \left[\left(i - \frac{2\Delta_n}{\Gamma_0} \right) \mathbb{1} - \frac{2\Delta_B}{\Gamma_0} \begin{pmatrix} -1 & 0 & 0 \\ 0 & 0 & 0 \\ 0 & 0 & 1 \end{pmatrix} \right] \delta_{nn'} \\ &\quad - \frac{6\pi}{k_0} (1 - \delta_{nn'}) \hat{d} \hat{G}(\mathbf{r}_n - \mathbf{r}_{n'}) \hat{d}^\dagger \end{aligned} \quad (1)$$

where $\Delta_B = g_e \mu_B B / \hbar$ is the Zeeman shift, μ_B is the Bohr magneton, g_e is the Landé factor of the excited state, $\mathbb{1}$ is the 3×3 identity matrix,

$$\hat{G}(\mathbf{r}) = -\frac{e^{ik_0 r}}{4\pi r} \left[P(ik_0 r) \mathbb{1} + Q(ik_0 r) \frac{\mathbf{r} \otimes \mathbf{r}}{r^2} \right] \quad (2)$$

is the dyadic Green's function of Maxwell equations with $k_0 = \omega_0/c = 2\pi/\lambda_0$, $P(u) = 1 - 1/u + 1/u^2$, $Q(u) = -1 + 3/u - 3/u^2$, and the matrix

$$\hat{d} = \begin{pmatrix} 1/\sqrt{2} & i/\sqrt{2} & 0 \\ 0 & 0 & 1 \\ -1/\sqrt{2} & i/\sqrt{2} & 0 \end{pmatrix} \quad (3)$$

converts the Green's tensor from the Cartesian coordinate basis to the so-called cyclic one [24, 42]. Following

previous works [22–26], we restrict our consideration to states in which no more than one excitation (photon) is present in the system, which corresponds to the one-particle setting suitable for discussing the Anderson localization phenomenon.

To study the optical transport through the system described by the Hamiltonian (1), we assume that the atomic sample has a shape of cylinder of radius R and height $L \ll R$. If the sample is illuminated by a monochromatic plane wave $\mathbf{E}_0(\mathbf{r}) \exp(-i\omega t) = \mathbf{u}_0 E_0 \exp(ikz - i\omega t)$ incident on its face $z = 0$, the vector $\beta_n = \{\beta_{nm}\}$ of probability amplitudes for the atom n to be excited in a state $|e_m\rangle$ obeys [31, 43, 44]

$$\begin{aligned} \frac{\partial \beta_n(t)}{\partial t} &= \left[i(\delta\omega - \Delta_n) - \frac{\Gamma_0}{2} \right] \beta_n(t) + \frac{id}{2\hbar} \hat{d} \mathbf{E}_0(\mathbf{r}_n) \\ &\quad - i \frac{3\pi\Gamma_0}{k_0} \sum_{n' \neq n}^N \left[\hat{d} \hat{G}(\mathbf{r}_n - \mathbf{r}_{n'}) \hat{d}^\dagger \right] \beta_{n'}(t) \end{aligned} \quad (4)$$

where $\delta\omega = \omega - \omega_m$ is the detuning of the incident light with respect to one of the Zeeman-shifted resonance frequencies $\omega_m = \omega_0 \pm m\Delta_B$, $m = \pm 1$. We model atomic motion as oscillations about random equilibrium positions $\mathbf{r}_n^{(0)}$ at a fixed frequency Ω : $r_{n\mu} = r_{n\mu}^{(0)} + A_{n\mu} \cos(\Omega t + \varphi_{n\mu})$, $\mu = x, y, z$, with random, normally distributed amplitudes $A_{n\mu}$, $\langle A_{n\mu} \rangle = 0$, $\langle A_{n\mu}^2 \rangle = A^2$, and phases $\varphi_{n\mu}$ uniformly distributed between 0 and 2π . Random frequency shifts Δ_n responsible for inhomogeneous broadening of atomic spectral lines are taken from a centered normal distribution with a variance Δ_0^2 . We find the stationary solution of Eq. (4) and compute the electric field outside the atomic sample

$$\mathbf{E}(\mathbf{r}, t) = \mathbf{E}_0(\mathbf{r}) - 4\pi d k_0^2 \sum_{n=1}^N \hat{G}(\mathbf{r} - \mathbf{r}_n) \hat{d}^\dagger \beta_n(t) \quad (5)$$

and the time-averaged transmission coefficient

$$\langle T \rangle = \frac{\Omega}{2\pi A |E_0|^2} \left\langle \int_0^{2\pi/\Omega} dt \int_A d^2\mathbf{r} |\mathbf{E}(\mathbf{r}, t)|^2 \right\rangle \quad (6)$$

where the spatial integration is over a disk of area $A = \pi(R/2)^2$ in a distant plane $z = L + 12/k_0$ and with a center on the z axis, angular brackets denote averaging over random sets of equilibrium positions $\{\mathbf{r}_n^{(0)}\}$, amplitudes $\{A_{n\mu}\}$ and phases $\{\varphi_{n\mu}\}$ of atomic oscillations. The polarization of the incident light is set to be circular with a chirality required to excite the transition $|g\rangle \rightarrow |e_m\rangle$ under study.

The dependence of the average dimensionless conductance $\langle g \rangle = (k_0 L)^2 \langle T \rangle$ on L witnesses whether the propagation of light is diffusive ($\langle g \rangle$ increases with L) or Anderson localization takes place ($\langle g \rangle$ decreases with L) [45]. Figure 1 shows dependencies of $\langle g \rangle$ on L for several sets of parameters and leads us to several important conclusions. First, Fig. 1(a) illustrates that the impact of atomic oscillations is negligible in both diffusion (the upper blue and green lines) and localization (the lower red line) regimes

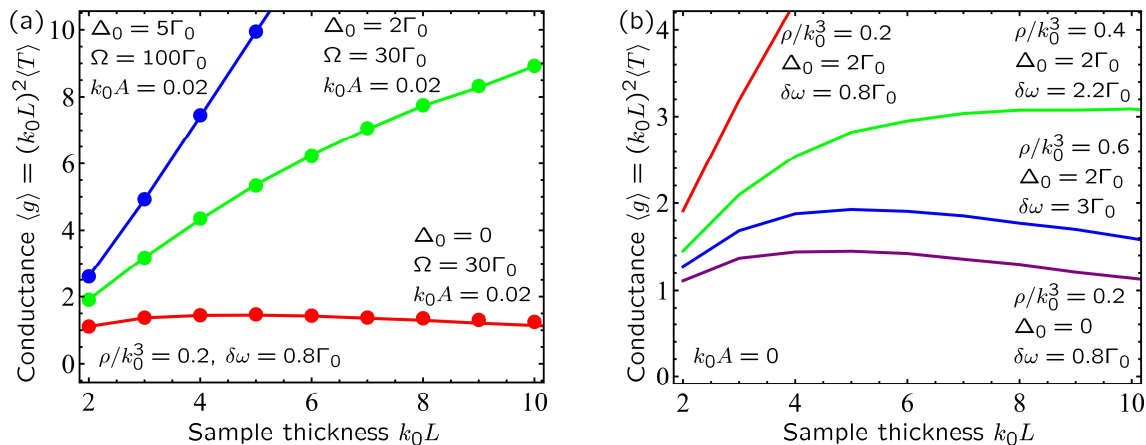


FIG. 1. Average dimensionless conductance $\langle g \rangle$ as a function of sample thickness L , for different parameters. Full circles result from full dynamic calculations taking into account fast oscillations of impurity atoms around random equilibrium positions with frequency Ω and amplitudes $A_{n\mu} \sim \mathcal{N}(0, A)$, as well as random frequency shifts of impurity resonant frequencies $\Delta_n \sim \mathcal{N}(0, \Delta_0)$. Solid lines are obtained by neglecting oscillations ($A = 0$).

of propagation. This can be understood by analogy with the so-called Dicke effect that consists in narrowing of atomic spectral lines in the presence of inter-atomic collisions: when the mean free path of atoms between two collisions becomes much shorter than the wavelength of light, the atomic line width becomes insensitive to the Doppler effect [37]. In our case, oscillations of atoms replace their random displacements due to collisions, and the condition of insensitivity of our results to the oscillations becomes $k_0 A \ll 1$. In the following, we assume that this condition is fulfilled and neglect atomic oscillations. Next, Fig. 1(b) shows that the destructive effect of inhomogeneous broadening on localization can be mitigated by increasing the atomic number density ρ and adjusting the detuning $\delta\omega$. In particular, whereas the lower (violet) line obtained in the absence of inhomogeneous broadening ($\Delta_0 = 0$) decays with $k_0 L$ for $k_0 L \gtrsim 4$ indicating Anderson localization, the upper (red) line obtained for exactly the same parameters except for $\Delta_0 = 2\Gamma_0$, grows with $k_0 L$ signaling that Anderson localization is suppressed by the inhomogeneous broadening. However, when we keep Δ_0 constant and increase the atomic number density ρ adjusting the frequency detuning $\delta\omega$, the curve $\langle g(k_0 L) \rangle$ bends down and approaches the one in the absence of broadening [see the two intermediate green and blue curves in Fig. 1(b)]. Whereas increasing ρ may be difficult for cold-atom systems, it is not necessarily the same for solid-state samples with embedded impurities, which gives hope for observation of Anderson localization of light in such samples despite the inhomogeneous broadening phenomenon.

In addition to the dependence of dimensionless conductance on sample thickness, a signature of Anderson localization can be found in the dependence of the average atomic excitation $\langle |\beta_n(t)|^2 \rangle$, with the averaging also over time t , on the depth z inside the sample [28], see Fig. 2. All curves in Fig. 2 correspond to atomic densities ρ for which Anderson localization is expected at $\delta\omega/\Gamma_0 = 0.8$ for $\Delta_0 = 0$ [24, 25]. We thus expect a

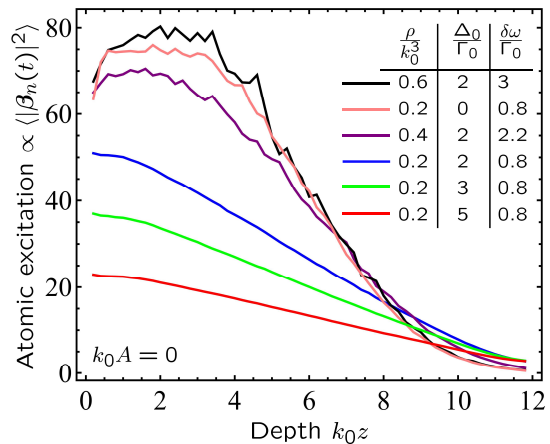


FIG. 2. Average profiles of atomic excitation inside a sample of thickness $k_0 L = 12$.

step-like (steep in the middle of the sample and flattened towards $z = 0$ and L) profile of $\langle |\beta_n(t)|^2 \rangle$ illustrated by the brown curve in Fig. 2 [28]. However, it is clear that the three lower curves obtained for the same ρ and $\delta\omega$ as the brown curve but in the presence of inhomogeneous broadening $\Delta_0 \geq 2$, exhibit a roughly linear decay with z characteristic of photon diffusion [23, 28]. Thus, the inhomogeneous broadening suppresses Anderson localization. Nevertheless, similarly to what has been discussed in connection with Fig. 1, this suppression can be mitigated and even fully canceled by increasing ρ and adjusting $\delta\omega$, as clearly witnessed by the violet and black curves in Fig. 2 that exhibit the shape expected for Anderson localization.

To gain a systematic understanding of the impact of inhomogeneous broadening on Anderson localization, we consider random distributions of $N \gg 1$ atoms in a sphere of diameter L and compute the complex eigenenergies E_n of the effective Hamiltonian (1), ordered by their real parts, see Supplementary Information (SI) [46] for details. They define frequencies $\omega_n = \omega_0 - (\Gamma_0/2)\text{Re}E_n$ and decay rates $\Gamma_n = \Gamma_0\text{Im}E_n$ of quasismodes of the

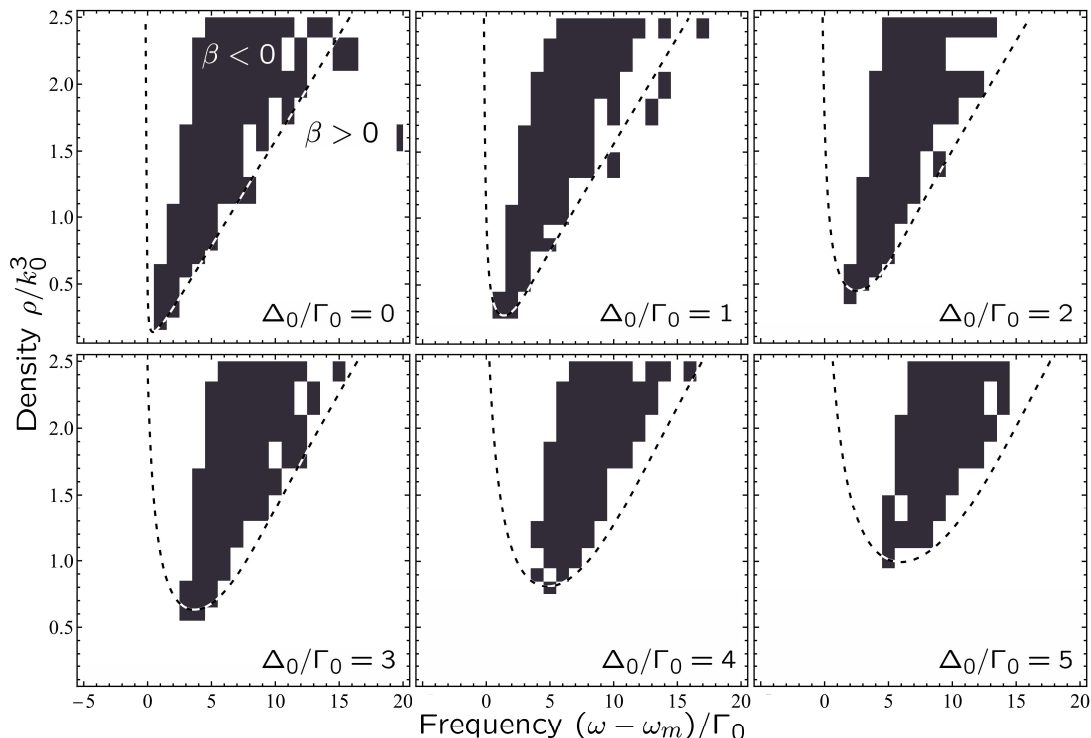


FIG. 3. Localization phase diagram for light in a large ensemble of $N \gg 1$ resonant scattering centers embedded in a solid matrix for six different values of inhomogeneous broadening Δ_0 . β -function (approximated by a finite difference from numerical results for $N = 8$ and 16×10^3) is negative and eigenstates are localized in the regions of the phase plane shown in black, whereas $\beta > 0$ and states are extended in the rest of the plane. Dashed lines show the mobility edge $\beta = 0$ predicted by our approximate analytic theory.

atomic system. Frequency-dependent Thouless conductance is defined as $g_{\text{Th}}(\omega) = \langle 1/\Gamma_n \rangle_\omega^{-1} / \langle \omega_n - \omega_{n-1} \rangle_\omega$ [22, 47] with averaging $\langle \dots \rangle_\omega$ over random realizations of atomic positions $\{\mathbf{r}_n\}$, frequency shifts $\{\Delta_n\}$ and, in addition, eigenenergies E_n for which ω_n fall inside a frequency interval of width Γ_0 around ω . To characterize the dependence of g_{Th} on L , we compute $\beta(g_{\text{Th}}) = \partial \ln g_{\text{Th}} / \partial \ln(k_0 L)$. $\beta > 0$ in the region of parameters for which quasimodes are extended in space whereas $\beta < 0$ for spatially localized eigenmodes [22, 45]. Figure 3 shows localization phase diagrams for light in the large ensemble of resonant scattering centers for different strengths of the inhomogeneous broadening Δ_0 . For $\Delta_0 = 0$, Anderson localization is expected in a certain range of frequencies only when $\rho/k_0^3 \gtrsim 0.1$ [25]. In agreement with our previous discussion, increasing Δ_0 leads to a requirement of higher density to reach localization but does not fully suppress it. An additional illustration of this is provided by Fig. 4 that shows the minimum density at which Anderson localization takes place in our model at any frequency, as a function of Δ_0 . The minimum density increases with Δ_0 but remains finite.

A simple interpretation of results shown in Figs. 3 and 4 can be obtained by averaging the self-energy $\Sigma(\omega)$ obtained in the independent scattering approximation (ISA) [48] over the normal distribution of resonance frequencies ω_{nm} of individual atoms, see SI [46]. The variance of the distribution is assumed to be equal to a sum of Δ_0^2 due to the random local electric fields and

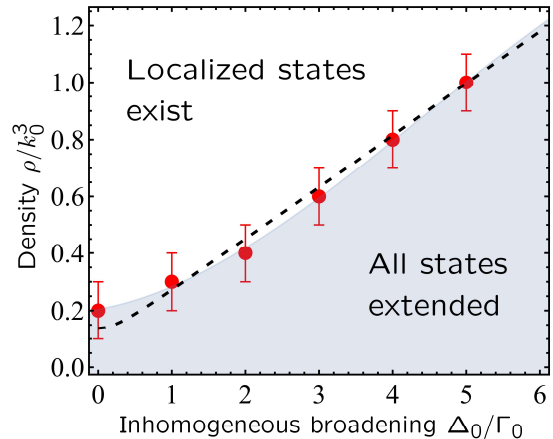


FIG. 4. Minimum number density of impurity atoms ρ required for collective atomic states to be spatially localized in some frequency band, as a function of the magnitude of inhomogeneous broadening Δ_0 (red disks with error bars). Grey shading shows the region of the parameter space in which all states are extended. Dashed line is the prediction of our approximate analytic theory.

a term $\sim (\rho/k_0^3)^2$ due to dipole-dipole interactions between nearby atoms [46]. This turns out to be a simple yet efficient way of taking into account the two effects otherwise neglected by ISA. We define the effective wave number $k_{\text{eff}} = \text{Re} \sqrt{k_0^2 - \langle \Sigma(\omega) \rangle}$ and the scattering mean free path $\ell = 1/2 \text{Im} \sqrt{k_0^2 - \langle \Sigma(\omega) \rangle}$. The Ioffe-Regel criterion of localization yields a simple condition for the

mobility edge : $k_{\text{eff}}\ell = (k_{\text{eff}}\ell)_c \sim 1$ [48–50]. Dashed lines in Fig. 3 show contour plots of this equation for different Δ_0 with $(k_{\text{eff}}\ell)_c = 0.6$. It captures the main tendency exhibited by the numerical results when Δ_0 increases although it is clearly not exact. An even better agreement is obtained for the minimum density required to reach localization in Fig. 4.

In conclusion, we demonstrate that transparent solids with impurity atoms or ions at random positions are promising materials for reaching Anderson localization of light in 3D. On the one hand, the detrimental effect of longitudinal optical fields [22, 23] can be mitigated in these materials by an external magnetic field, in the same way as in cold-atom systems [24, 25], which gives them an advantage over suspensions or powders of dielectric particles [10, 11]. On the other hand, they do not suffer from strong losses characteristic of metallic structures proposed as candidates for observation of Anderson localization of light [12, 18]. The main result of this work is to show that the difficulties specific for solids with impurity atoms—the oscillations of impurity atoms about their equilibrium positions and the inhomogeneous broadening of their spectra due to random local electric fields—are not critical and should not impede observation of Anderson localization of light. Therefore, we believe that it would be worthwhile to put some effort in experimenting with such materials.

The work of IMS was supported by the Foundation for the Advancement of Theoretical Physics and Mathematics “BASIS”. Calculations were performed using the computing resources of the supercomputer center of Peter the Great St. Petersburg Polytechnic University.

* Sergey.Skipetrov@lpmmc.cnrs.fr

† igor.m.sokolov@gmail.com

- [1] P. W. Anderson, *Phys. Rev.* **109**, 1492 (1958).
- [2] D. S. Wiersma, P. Bartolini, A. Lagendijk, and R. Righini, *Nature* **390**, 671 (1997).
- [3] F. Scheffold, R. Lenke, R. Tweer, and G. Maret, *Nature* **398**, 206 (1999).
- [4] D. S. Wiersma, J. G. Rivas, P. Bartolini, A. Lagendijk, and R. Righini, *Nature* **398**, 207 (1999).
- [5] T. van der Beek, P. Barthelemy, P. M. Johnson, D. S. Wiersma, and A. Lagendijk, *Phys. Rev. B* **85**, 115401 (2012).
- [6] M. Störzer, P. Gross, C. M. Aegerter, and G. Maret, *Phys. Rev. Lett.* **96**, 063904 (2006).
- [7] T. Sperling, W. Bührer, C. M. Aegerter, and G. Maret, *Nat. Photon.* **7**, 48 (2013).
- [8] F. Scheffold and D. Wiersma, *Nat. Photon.* **7**, 934 (2013).
- [9] G. Maret, T. Sperling, W. Bührer, A. Lubatsch, R. Frank, and C. M. Aegerter, *Nat. Photon.* **7**, 934 (2013).
- [10] T. Sperling, L. Schertel, M. Ackermann, G. Aubry, C. Aegerter, and G. Maret, *New J. Phys.* **18**, 013039 (2016).
- [11] S. E. Skipetrov and J. H. Page, *New J. Phys.* **18**, 021001 (2016).
- [12] A. Yamilov, S. E. Skipetrov, T. W. Hughes, M. Minkov, Z. Yu, and H. Cao, *Nat. Phys.* **19**, 1308 (2023).
- [13] S. John, *Phys. Rev. Lett.* **58**, 2486 (1987).
- [14] S. John, *Physics Today* **44**(5), 32 (1991).
- [15] S. John, in *Photonic Band Gaps and Localization*, edited by C. Soukoulis (Plenum Press, New York, 1993) pp. 1–22.
- [16] J. Haberko, L. S. Froufe-Pérez, and F. Scheffold, *Nat. Comm.* **11**, 4867 (2020).
- [17] F. Scheffold, J. Haberko, S. Magkiriadou, and L. S. Froufe-Pérez, *Phys. Rev. Lett.* **129**, 157402 (2022).
- [18] A. Z. Genack and N. Garcia, *Phys. Rev. Lett.* **66**, 2064 (1991).
- [19] A. A. Chabanov, M. Stoytchev, and A. Z. Genack, *Nature* **404**, 850 (2000).
- [20] R. Kaiser, in *Peyresq Lectures on Nonlinear Phenomena*, Vol. 1, edited by R. Kaiser and J. Montaldi (World Scientific, Singapore, 2000) pp. 95–126.
- [21] R. Kaiser, *J. Mod. Opt.* **56**, 2082 (2009).
- [22] S. E. Skipetrov and I. M. Sokolov, *Phys. Rev. Lett.* **112**, 023905 (2014).
- [23] B. A. van Tiggelen and S. E. Skipetrov, *Phys. Rev. B* **103**, 174204 (2021).
- [24] S. E. Skipetrov and I. M. Sokolov, *Phys. Rev. Lett.* **114**, 053902 (2015).
- [25] S. E. Skipetrov, *Phys. Rev. Lett.* **121**, 093601 (2018).
- [26] S. E. Skipetrov, I. M. Sokolov, and M. D. Havey, *Phys. Rev. A* **94**, 013825 (2016).
- [27] F. Cottier, A. Cipris, R. Bachelard, and R. Kaiser, *Phys. Rev. Lett.* **123**, 083401 (2019).
- [28] S. E. Skipetrov and I. M. Sokolov, *Phys. Rev. Lett.* **123**, 233903 (2019).
- [29] R. Kaiser and M. Havey, *Opt. Photon. News* **16**, 38 (2005).
- [30] W. Guerin, M. Araújo, and R. Kaiser, *Phys. Rev. Lett.* **116**, 083601 (2016).
- [31] A. S. Kuraptsev and I. M. Sokolov, *Phys. Rev. A* **101**, 033602 (2020).
- [32] C. Hahlweg, W. Zhao, and H. Rothe, in *Novel Optical Systems Design and Optimization XV*, Vol. 8487, edited by G. G. Gregory and A. J. Davis, International Society for Optics and Photonics (SPIE, 2012) p. 84870S.
- [33] J. Koo, L. R. Walker, and S. Geschwind, *Phys. Rev. Lett.* **35**, 1669 (1975).
- [34] S. Chu, H. M. Gibbs, S. L. McCall, and A. Passner, *Phys. Rev. Lett.* **45**, 1715 (1980).
- [35] I. Aharonovich, A. D. Greentree, and S. Praver, *Nat. Photon.* **5**, 397 (2011).
- [36] M. W. Doherty, N. B. Manson, P. Delaney, F. Jelezko, J. Wrachtrup, and L. C. Hollenberg, *Phys. Rep.* **528**, 1 (2013).
- [37] R. H. Dicke, *Phys. Rev.* **89**, 472 (1953).
- [38] C. Cohen-Tannoudji, J. Dupont-Roc, and G. Grynberg, *Photons and Atoms-Introduction to Quantum Electrodynamics* (Wiley Science Papers Series, New York, 1992).
- [39] O. Morice, Y. Castin, and J. Dalibard, *Phys. Rev. A* **51**, 3896 (1995).
- [40] R. H. Lehmann, *Phys. Rev. A* **2**, 883 (1970).
- [41] G. S. Agarwal, *Phys. Rev. A* **2**, 2038 (1970).
- [42] D. A. Varshalovich, A. N. Maskalev, and V. K. Khersonskii, *Quantum Theory of Angular Momentum* (World Scientific, Singapore, 1988).
- [43] P. W. Courteille, S. Bux, E. Lucioni, K. Lauber, T. Bienaimé, R. Kaiser, and N. Piovela, *Eur. Phys. J. D* **58**, 69 (2010).
- [44] I. M. Sokolov, D. V. Kupriyanov, and M. D. Havey, *J. Exp. Theor. Phys.* **112**, 246 (2011).
- [45] E. Abrahams, P. W. Anderson, D. C. Licciardello, and T. V. Ramakrishnan, *Phys. Rev. Lett.* **42**, 673 (1979).

- [46] Supplementary information, `URL_will_be_inserted_by_publisher`.
- [47] J. Wang and A. Z. Genack, *Nature* **471**, 345 (2011).
- [48] P. Sheng, *Introduction to Wave Scattering, Localization and Mesoscopic Phenomena*, 2nd ed. (Springer-Verlag, Berlin, 2006).
- [49] A. F. Ioffe and A. R. Regel, in *Progress in Semiconductors*, edited by A. F. Gibson (Wiley, New York, 1960) pp. 237–291.
- [50] S. E. Skipetrov and I. M. Sokolov, *Phys. Rev. B* **98**, 064207 (2018).

Supplementary information for “Anderson localization of light by impurities in a solid transparent matrix”

S.E. Skipetrov
Univ. Grenoble Alpes, CNRS, LPMMC, 38000 Grenoble, France
E-mail: Sergey.Skipetrov@lpmmc.cnrs.fr

I.M. Sokolov
Peter the Great St. Petersburg Polytechnic University, 195251 St. Petersburg, Russia
E-mail: igor.m.sokolov@gmail.com

DETAILS OF THE SCALING ANALYSIS

We generate independent spatial configurations of N atoms randomly distributed inside a sphere of diameter L at a number density $\rho = N/V$ with $V = \pi L^3/6$. For each atom, a random shift Δ_n of its resonance frequency ω_0 is sampled from a centered normal distribution with variance Δ_0^2 . For each atomic configuration with a corresponding set of Δ_n , complex eigenvalues E_n of the effective Hamiltonian (1) are computed numerically and ordered according to their real parts. Then, mean values of $1/\Gamma_n$ and of $\omega_n - \omega_{n-1}$ are computed in each frequency interval of width Γ_0 from $\delta\omega = \omega - \omega_m = -5\Gamma_0$ to $20\Gamma_0$, where $\omega_n = \omega_0 - (\Gamma_0/2)\text{Re}E_n$ and $\Gamma_n = \Gamma_0\text{Im}E_n$. Averaging is also performed over a large number of independent atomic configurations in space and over $\{\Delta_n\}$. Typically, we average over 50, 35 and 25 configurations for $N = 8000, 12000$ and 16000 , respectively. Thouless conductance is defined as $g_{\text{Th}}(\omega) = \langle 1/\Gamma_n \rangle_{\omega}^{-1} / \langle \omega_n - \omega_{n-1} \rangle_{\omega}$, where the notation $\langle \dots \rangle_{\omega}$ highlights the additional averaging over all ω_n inside an interval of width Γ_0 around the frequency ω .

Figure S1 shows g_{Th} as a function of $k_0\ell_0 = k_0^3/6\pi\rho$ and $\delta\omega/\Gamma_0$, for six different values of Δ_0 . It is clear that the drop of g_{Th} around $\delta\omega/\Gamma_0 = 4$ at $\Delta_0 = 0$, shifts to larger $\delta\omega$ and becomes less pronounced with increasing Δ_0 . The impact of inhomogeneous broadening on Thouless conductance at a given frequency is demonstrated in Fig. S2 for $\delta\omega/\Gamma_0 = 4$. When $\Delta_0 < 4$, localization transitions take place at values of $k_0\ell_0$ where curves corresponding to different N cross. These transitions are suppressed for $\Delta_0 > 4$, leading to g_{Th} being a growing function of N at all densities ρ . Figure 4 of the main text is obtained by estimating the β -function $\beta(g_{\text{Th}}) = \partial \ln g_{\text{Th}} / \partial \ln(k_0L)$ using a finite-difference approximation for the derivative.

INFLUENCE OF INHOMOGENEOUS BROADENING ON ANDERSON LOCALIZATION OF LIGHT IN COLD ATOMIC CLOUDS: APPROXIMATE ANALYTIC THEORY

In the independent scattering approximation, the self-energy is [21, 48]

$$\Sigma(\omega, \omega'_0) = \frac{4\pi\rho}{k_0} \times \frac{1}{2(\omega - \omega'_0)/\Gamma_0 + i} \quad (\text{S1})$$

We assume that the atomic resonance frequency ω'_0 is subject to inhomogeneous broadening due to (i) strong local fields in the transparent host medium and (ii) strong dipole-dipole interactions between nearby atoms. The resulting distribution of ω'_0 is approximated by a Gaussian:

$$p(\omega'_0) = \frac{1}{\sqrt{2\pi}\Delta} \exp\left[-\frac{(\omega'_0 - \omega_0)^2}{2\Delta^2}\right] \quad (\text{S2})$$

where ω_0 is the resonance frequency in the absence of broadening. The variance of the distribution (S2) is given by a sum of two contributions:

$$\Delta^2 = \Delta_0^2 + \langle \Delta_{\text{dd}}^2 \rangle \quad (\text{S3})$$

First, local fields in the host crystal yield random frequency shifts that we denote by Δ_n , with a variance Δ_0^2 . Second, the typical frequency shifts Δ_{dd} induced by dipole-dipole interactions are of the order of $1/(k_0\Delta r)^3 \propto \rho/k_0^3$, where we used the fact that the typical distance between nearby atoms is $\Delta r = \rho^{-1/3}$. To obtain a quantitative estimate, we recall that in a strong magnetic field, the eigenvalues of the Hamiltonian (1) in the main text, yielding eigenfrequencies ω near resonances ω_m ($m = \pm 1$), can be obtained by diagonalizing a $N \times N$ matrix [24, 25]

$$\begin{aligned} (\hat{H}_{\text{eff}})_{nn'} &= \left(i \mp 2 \frac{\Delta_B}{\Gamma_0}\right) \delta_{nn'} + (1 - \delta_{nn'}) \frac{3}{2} \frac{e^{ik_0\Delta r_{nn'}}}{k_0\Delta r_{nn'}} \\ &\times \left[P(ik_0\Delta r_{nn'}) + Q(ik_0\Delta r_{nn'}) \frac{\sin^2 \theta_{nn'}}{2} \right] \end{aligned} \quad (\text{S4})$$

where $\theta_{nn'}$ is the angle between the vector $\Delta \mathbf{r}_{nn'} = \mathbf{r}_n - \mathbf{r}_{n'}$ and the quantization axis z . To be specific, let us consider $m = 1$. For two atoms ($N = 2$) at a distance $\Delta \mathbf{r} = \mathbf{r}_2 - \mathbf{r}_1$ the two eigenvalues of the matrix (S4) are

$$\begin{aligned} E_{\pm} &= \left(i - 2 \frac{\Delta_B}{\Gamma_0}\right) \pm \frac{3}{2} \frac{e^{ik_0\Delta r}}{k_0\Delta r} \\ &\times \left[P(ik_0\Delta r) + Q(ik_0\Delta r) \frac{\sin^2 \theta}{2} \right] \end{aligned} \quad (\text{S5})$$

and frequency shifts with respect to $\omega_1 = \omega_0 + \Delta_B$ are $(\Delta_{\text{dd}})_{\pm} = -(\Gamma_0/2)\text{Re}E_{\pm} - \Delta_B$. Averaging over the two eigenvalues and over θ yields

$$\langle \Delta_{\text{dd}} \rangle = 0 \quad (\text{S6})$$

$$\begin{aligned}
\langle \Delta_{\text{dd}}^2 \rangle &= \frac{3}{160} \left(\frac{\rho}{k_0^3} \right)^{\frac{2}{3}} \left\{ 3 \left(\frac{\rho}{k_0^3} \right)^{\frac{4}{3}} + \left(\frac{\rho}{k_0^3} \right)^{\frac{2}{3}} \right. \\
&+ \left[3 \left(\frac{\rho}{k_0^3} \right)^{\frac{4}{3}} - 5 \left(\frac{\rho}{k_0^3} \right)^{\frac{2}{3}} + 7 \right] \cos \left[2 \left(\frac{\rho}{k_0^3} \right)^{-\frac{1}{3}} \right] \\
&+ \left. \left[6 \left(\frac{\rho}{k_0^3} \right) - 2 \left(\frac{\rho}{k_0^3} \right)^{\frac{1}{3}} \right] \sin \left[2 \left(\frac{\rho}{k_0^3} \right)^{-\frac{1}{3}} \right] + 7 \right\} \\
&\rightarrow \frac{9}{80} \left(\frac{\rho}{k_0^3} \right)^2
\end{aligned} \tag{S7}$$

where in the last line we have taken the limit $\rho/k_0^3 \gg 1$.

The average self-energy is

$$\langle \Sigma(\omega, \omega_0) \rangle = \int_{-\infty}^{\infty} d\omega' p(\omega') \Sigma(\omega, \omega') \tag{S8}$$

The effective complex wave number is

$$\sqrt{k_0^2 - \langle \Sigma(\omega, \omega_0) \rangle} = k + \frac{i}{2\ell} \tag{S9}$$

and hence

$$k = \text{Re} \sqrt{k_0^2 - \langle \Sigma(\omega, \omega_0) \rangle} \tag{S10}$$

$$\ell = \frac{1}{2 \text{Im} \sqrt{k_0^2 - \langle \Sigma(\omega, \omega_0) \rangle}} \tag{S11}$$

Ioffe-Regel criterion of localization is

$$k\ell = \frac{\text{Re} \sqrt{k_0^2 - \langle \Sigma(\omega, \omega_0) \rangle}}{2 \text{Im} \sqrt{k_0^2 - \langle \Sigma(\omega, \omega_0) \rangle}} = (k\ell)_c \sim 1 \tag{S12}$$

Comparison of contour plots of this equation with the localization phase diagram following from numerical calculations is shown in Fig. 3 of the main text.

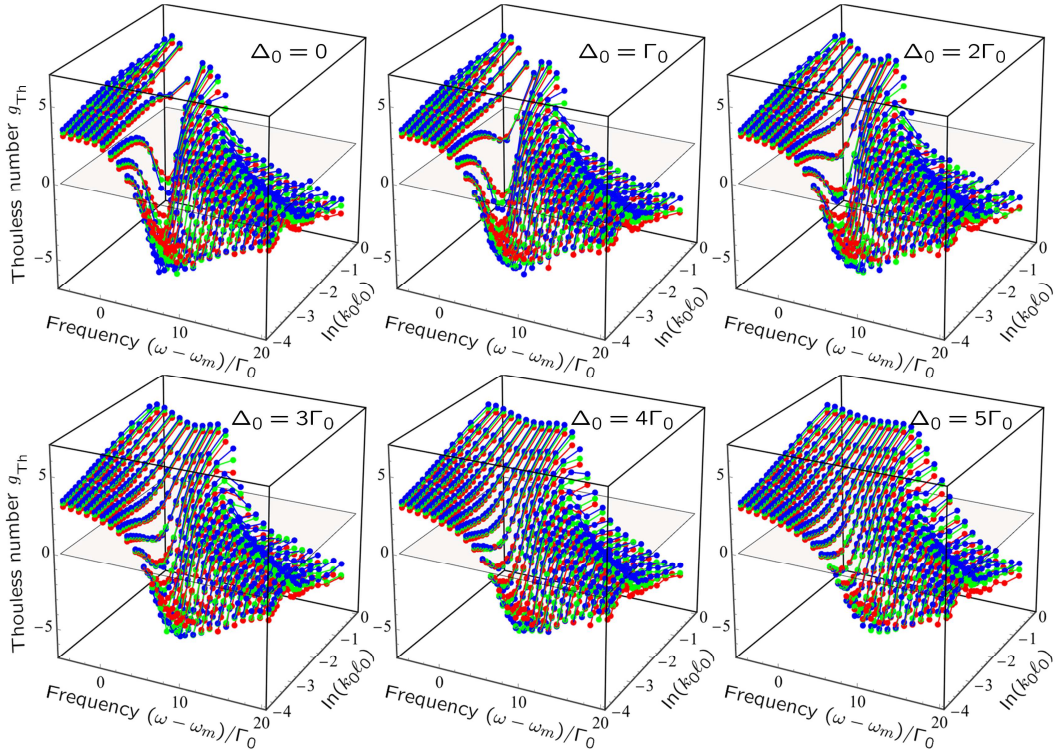


FIG. S1. Thouless conductance g_{Th} as a function of the bare Ioffe-Regel parameter $k_0 l_0 = k_0^3 / 6\pi\rho$ and frequency detuning $\delta\omega = \omega - \omega_m$, for six different values of inhomogeneous broadening Δ_0 . Data obtained for different total numbers of atoms are shown in different colors: $N = 8000$ (red), 12000 (green), 16000 (blue). The explored range of $k_0 l_0$ corresponds to the range $\rho/k_0^3 = 0.1$ –2.5 of the atomic number density.

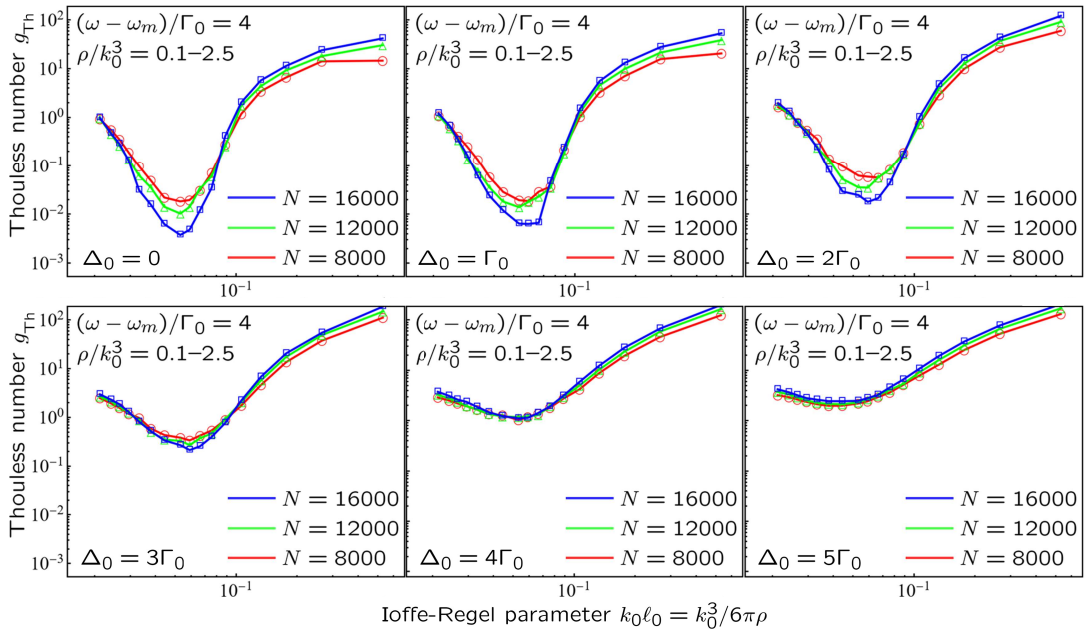


FIG. S2. A cut of Fig. S1 at $\delta\omega = \omega - \omega_m = 4\Gamma_0$, intended to demonstrate the transition from Anderson localization for $\Delta_0 < 4$ (curves corresponding to different N cross in points determining mobility edges) to diffuse transport for $\Delta_0 > 4$ (no crossings).